Unveiling the adsorption mechanism of zeolitic imidazolate framework-8 with high efficiency for removal of copper ions from aqueous solutions†

Yujie Zhang,‡[a] Zhiqiang Xie,‡[b] Zhuqing Wang,[a,c] Xuhui Feng,[d] Ying Wang*[b] and Aiguo Wu*[a]

Among the heavy metal ions, copper(II) can cause eye and liver damage at high uptake. The existence of copper ions (Cu^{2+}) even with an ultralow concentration of less than 0.1 μg g^{-1} can be toxic to living organisms. Thus, it is highly desirable to develop efficient adsorbents to remove Cu^{2+} from aqueous solutions. In this work, without any surface functionalization or pretreatment, a water-stable zeolitic imidazolate framework (ZIF-8) synthesized at room temperature is directly used as a highly efficient adsorbent for removal of copper ions from aqueous solutions. To experimentally unveil the adsorption mechanism of Cu^{2+} by using ZIF-8, we explore various effects from a series of important factors, such as pH value, contact time, temperature and initial Cu^{2+} concentration. As a result, ZIF-8 nanocrystals demonstrate an unexpected high adsorption capacity of Cu^{2+} and high removal efficiency for both high and low concentrations of Cu^{2+} from water. Moreover, ZIF-8 nanocrystals possess fast kinetics for removing Cu^{2+} with the adsorption time of less than 30 min. In addition, the pH of the solution ranging from 3 to 6 shows little effect on the adsorption of Cu^{2+} by ZIF-8. The adsorption mechanism is proposed for the first time and systematically verified by various characterization techniques, such as TEM, FTIR, XPS, XRD and SEM.

Introduction

With the rapid increase of industrial and human activities, disposal of industrial wastewater has become one of the most important environmental issues worldwide.[1,2] Heavy metal pollution has posed severe threat to the environment and public health since heavy metals are not biodegradable and are prone to accumulate in the environment. In addition, most of the heavy metal ions even with low concentrations are dangerous and extremely toxic to human health. For example, a high concentration of Cu^{2+} in public drinking water systems will result in serious diseases such as cramps, diarrhea, gastrointestinal catarrh and damage of the liver and kidney.[3,4] According to Environmental Protection Agency (EPA) guidelines and World Health Organization (WHO), the permissible limits of Cu^{2+} for drinking water quality are 1.3 and 2.0 mg L^{-1}, respectively.[5] Therefore, it is crucial to develop suitable methods to efficiently remove trace-level heavy metal ions from aqueous systems. To date, various approaches, such as chemical precipitation,[6,7] ion exchange,[8] membrane filtration,[9] and adsorption,[10–12] have been reported for heavy metal wastewater treatment. Among them, adsorption has been considered as an economic and effective approach for heavy metal wastewater treatment benefiting from its flexibility and simplicity of design, low operation cost and good adsorption capability. Furthermore, adsorption is partially reversible, and thus adsorbents sometimes can be recovered by a suitable desorption process. Among the available adsorbents, activated carbon (AC) and carbon nanotubes (CNTs) have been widely reported as promising adsorbents for the removal of heavy metal ions.[13–17] However, the adsorption capacities of metal ions by AC and CNTs are very low and the whole adsorption process usually takes several hours or even longer. Furthermore, both AC and CNTs are expensive, which further hinders their practical applications in heavy metal wastewater treatment. Recently, various nanosized metal oxides (NMOs),[18–22] such as nanosized Fe_3O_4, Fe_2O_3, TiO_2 and CeO_2, have been studied as prom-

[a]*Key Laboratory of Magnetic Materials and Devices & Key Laboratory of Additive Manufacturing Materials of Zhejiang Province & Division of Functional Materials and Nanodevices, Ningbo Institute of Materials Technology and Engineering, Chinese Academy of Sciences, Ningbo 315201, China. E-mail: aiguo@nimte.ac.cn; Fax: +86-574-86685163; Tel: +86-574-86685039*
[b]*Department of Mechanical & Industrial Engineering, Louisiana State University, Baton Rouge, LA 70803, USA. E-mail: ywang@lsu.edu*
[c]*Department of Chemistry, Anqing Normal College, Anqing, China*
[d]*Department of Chemical & Biological Engineering, Colorado School of Mines, Golden, Colorado 80401, USA*

ising alternatives for removal of heavy metal ions from aqueous systems owing to their high specific surface areas and high activities resulting from the so-called size-quantization effect. Nevertheless, NMOs tend to agglomerate owing to their high surface energy;[23–26] thus the adsorption capacity of NMOs would be significantly decreased. Therefore, it is highly challenging but extremely desirable to develop low-cost adsorbents with both high efficiency and high adsorption capacity for practical applications in the removal of heavy metals from industrial wastewater.

Metal organic frameworks (MOFs), as typical inorganic–organic hybrid crystalline solids with well-defined nanoporous structures, have been extensively applied for wide applications in gas separation,[27] sensors,[28] catalysis,[29] and drug delivery,[30] lithium ion batteries (LIBs)[31] and dye sensitized solar cells (DSSCs),[32] thanks to their high surface area and large porosity. In recent years, MOFs have drawn more and more attention as new adsorbents for applications in heavy metal wastewater treatment. For example, a metal–organic framework $Cu_3(BTC)_2$ with thio/thiol-functional groups has been reported for efficient removal of both mercury and lead ions.[33] Cu-based MOF $Cu_3(BTC)_2$ with sulfonic acid functional groups demonstrated high adsorption capability and selectivity of cadmium ions in water.[34] Zr-based MOFs were also reported for selective removal of Cu^{2+} over Ni^{2+} in water.[35] However, the aforementioned MOFs were mainly prepared using hydro/solvothermal, sonochemical and microwave methods, which generally require a time-consuming process, expensive equipment and/or a high temperature procedure. Furthermore, surface functionalization of MOFs with specific functional groups is usually needed for removal of heavy metal ions, which requires complicated, tedious processes and very careful control of reaction conditions such as the concentration of the reactants and pH value in the solutions, posing big challenges for potential large-scale production of highly efficient adsorbents.

In this work, water-stable zeolitic imidazolate framework (ZIF-8) nanocrystals synthesized at room temperature are tested for highly efficient removal of copper ions from aqueous systems. As a result, ZIF-8s demonstrate unexpectedly high removal efficiency and high adsorption capacities of Cu^{2+} over other heavy metal ions. The possible adsorption mechanism is explored for the first time using various characterization techniques, such as scanning electron microscopy (SEM), transmission electron microscopy (TEM), Fourier transform infrared spectroscopy (FTIR), X-ray photoelectron spectroscopy (XPS) and X-ray diffraction (XRD).

Results and discussion

Effect of pH

One of the major factors affecting the Cu^{2+} adsorption capacity and removal efficiency is the pH value of the solutions, since pH may not only change the speciation of metal ions, but also influence the structural stability and surface charges of the adsorbent. Therefore, 30 mL Cu^{2+} solution (120 mg L^{-1}) with the pH range of 2 to 6 is prepared; the adsorption time and temperature are fixed at 1 hour and 25 °C respectively. The effect of pH on the adsorption properties of ZIF-8 for Cu^{2+} is investigated as shown in Fig. 1a. The adsorption quantity increases significantly with the increase of the pH value from 2.5 to 3, and remains unchanged with further increase of the pH of the solution. It is found that only less than 20% Cu^{2+} is adsorbed when the pH of solutions is below 3. It might be attributed to protonation of the amino moiety of ZIF-8, which reduces the coordination ability between the nitrogen atom and Cu^{2+}.[36] It might also be due to the instability of ZIF-8 under strong acidic conditions. When the pH value is increased from 3 to 6, the adsorption quantity almost remains constant, indicating that the pH does not affect the adsorption properties of ZIF-8 under these conditions. However, when the pH is higher than 6, precipitation of cupric hydroxide may be formed with a higher concentration of Cu^{2+} (the Ksp of $Cu(OH)_2$ is 2.2×10^{-20}).[36] Therefore, the adsorption experiments are not investigated when the pH is higher than 6. Finally, the pH is optimized from 4 to 5 and ZIF-8 remains stable within this range. Moreover, neither protonation of the amine moiety nor precipitation of cupric hydroxide occurs, which is beneficial to the adsorption of Cu^{2+}. To further study the stability of a pure ZIF-8 sample in acid solutions, we tested and analyzed the concentrations of Zn^{2+} release in various aqueous solutions with different pH values using the inductively coupled plasma optical emission spectrometry (ICP-OES) technique. As shown in Fig. S1,† it is found that there is almost no Zn^{2+} release at pH 5–6, indicating that ZIF-8 is very stable in such a weak acid solution. Even in a strong acid solution at pH 3–4, only less than 10% of Zn^{2+} release occurs. However, in a stronger acid solution at pH 2, a high percentage of Zn^{2+} release (57%) is observed, suggesting that ZIF-8 would decompose in such a strong acid solution. Such results are consistent with the adsorption performances of ZIF-8 in the Cu^{2+} removal in aqueous solutions with pH values ranging from 2 to 6.

Effect of the contact time

The effect of contact time on the adsorption properties of ZIF-8 is investigated in a solution with a pH of 4 at 25 °C. As displayed in Fig. 1b, the rate of adsorption is very fast. The uptake of Cu^{2+} by ZIF-8 is 85% within 2 min, and reaches 95% in less than 10 min. The high adsorption rate of ZIF-8 is likely due to the high specific surface area of ZIF-8 (1340 m^2 g^{-1}, Fig. S2†) and a large number of amino moieties on the surface of ZIF-8.[37] To the best of our knowledge, such an impressive adsorption efficiency is much higher than the existing adsorbents for removal of Cu^{2+} from aqueous systems.[38–40] In order to make sure that the adsorption completed with a higher Cu^{2+} concentration, the contact time of 30 min is chosen.

Effect of temperature

The adsorption test is carried out in a range of 20–60 °C with the pH of 4, and the adsorption time and Cu^{2+} concentration are fixed at 30 min and 150 mg L^{-1} respectively. The effect of temperature on Cu^{2+} adsorption by ZIF-8 is shown in Fig. 1c

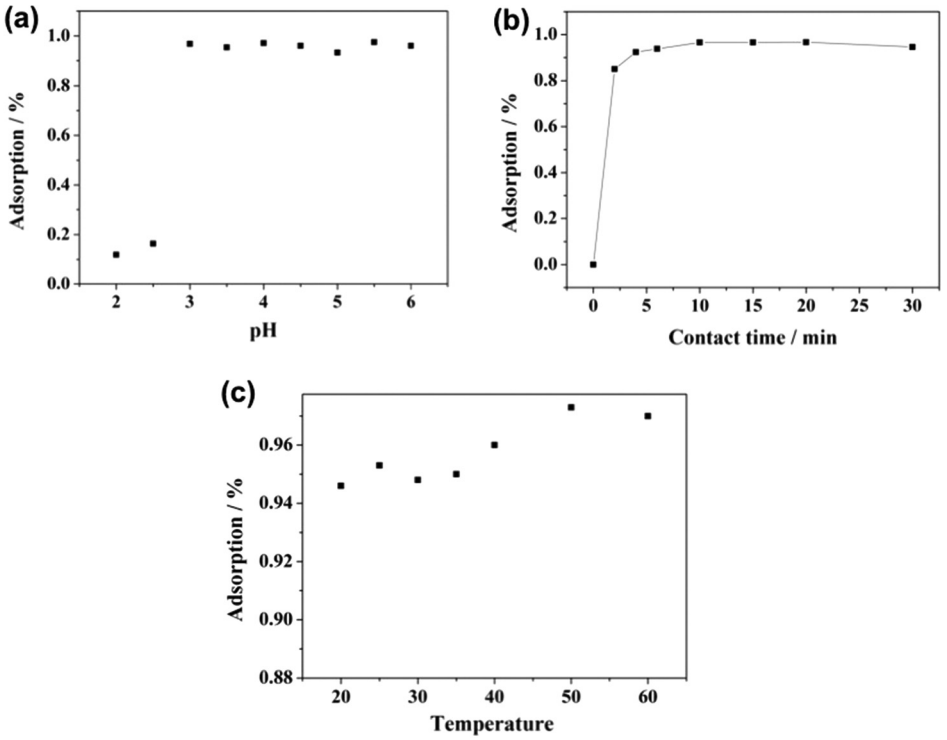

Fig. 1 Effect of pH, contact time and temperature on Cu^{2+} adsorption by ZIF-8 (initial Cu^{2+} concentration: 120 mg L^{-1}, 120 mg L^{-1} and 150 mg L^{-1} respectively).

from which we can observe that the adsorption quantity is almost the same from 20 to 35 °C and increases with the further increase of temperature from 35 to 50 °C, indicating that the adsorption process is an endothermic adsorption reaction.

Effect of the initial Cu^{2+} concentration

In order to determine the maximum adsorption capacity of ZIF-8, 10 mg ZIF-8 is equilibrated with 30 mL Cu^{2+} solutions with concentrations ranging from 2 to 420 mg L^{-1} for 30 min. The results in Fig. 2a show that the amount of Cu^{2+} adsorbed per unit mass of ZIF-8 (q, mg g^{-1}) increases with the increase of the initial concentration of Cu^{2+}. The obtained q value reaches approximately 800 mg g^{-1} when the initial concentration of Cu^{2+} is 420 mg L^{-1}, which is higher than most of the other adsorbents.[36,41,42] In order to ascertain the reason for the unexpected high q value, the solution after adsorption is analyzed in detail and the release of Zn^{2+} is found. In Fig. 2a, we can see that the released amount of Zn^{2+} increases with the increase of the Cu^{2+} concentration and then remains constant

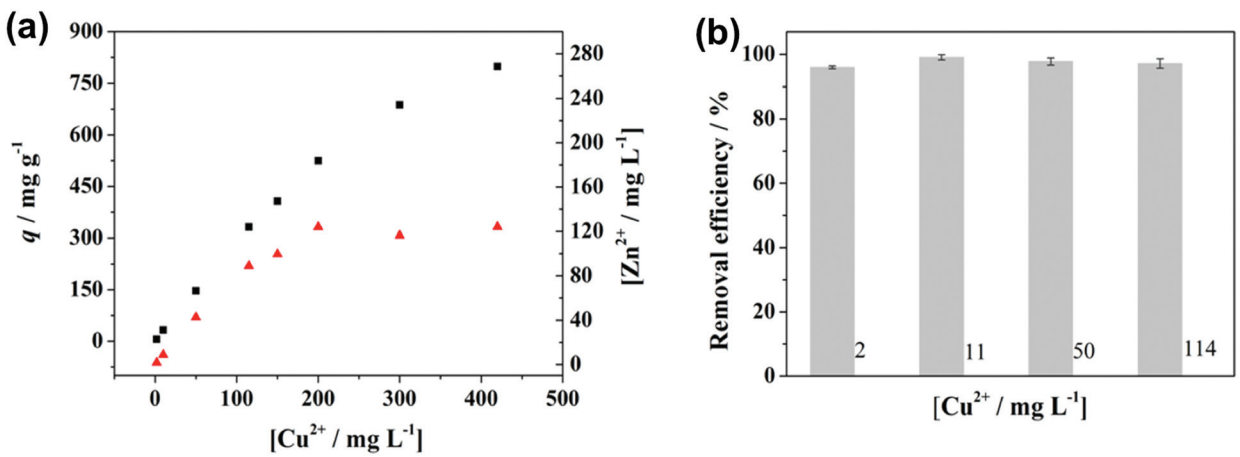

Fig. 2 Effect of the Cu^{2+} concentration on the q value of ZIF-8 (a, black), release of Zn^{2+} (a, red) and removal efficiency of Cu^{2+} (b).

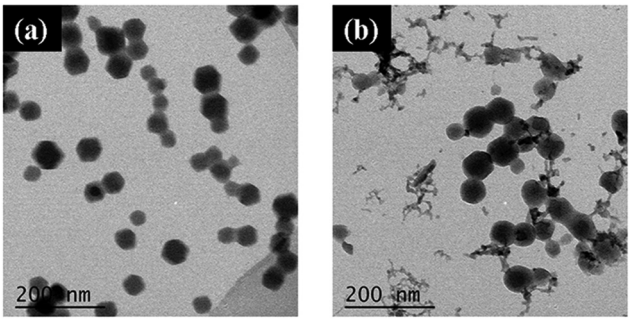

Fig. 3 TEM images of ZIF-8 (a) before and (b) after adsorption (Cu^{2+} concentration of 150 mg L^{-1}).

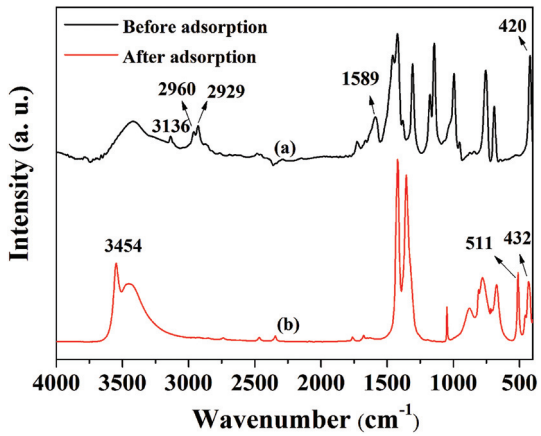

Fig. 4 FTIR spectra of ZIF-8 (a) before and (b) after adsorption (Cu^{2+} concentration of 150 mg L^{-1}).

until the Cu^{2+} concentration is more than 200 mg L^{-1}, which reveals that Zn^{2+} in ZIF-8 has been completely replaced by Cu^{2+}. However, the q value of ZIF-8 increases continually as the Cu^{2+} concentration increases from 200 to 420 mg L^{-1}, which is likely due to the coordination reaction between Cu^{2+} and the nitrogen atom on 2-methylimidazole.[5] Under optimal experimental conditions (time = 30 min, pH = 4), when the initial concentration of Cu^{2+} is 114 mg L^{-1}, the removal efficiency of Cu^{2+} is up to 97.2% (Fig. 2b). Moreover, when the initial concentration of Cu^{2+} is 2 mg L^{-1}, the removal efficiency is up to 96% and the remaining concentration of Cu^{2+} is 0.085 mg L^{-1}, which is much lower than the maximum allowed concentration of Cu^{2+} in drinking water defined by the US EPA (1.3 mg L^{-1}). These results demonstrate that the as-prepared ZIF-8 is applied to treat wastewater with both high and low concentrations, which is an important indicator for good adsorbents.

Investigation of the mechanism of adsorption

TEM analysis. The structure of ZIF-8 before and after adsorption is characterized by TEM as shown in Fig. 3. Before adsorption, ZIF-8 is a hexagonal structure with a particle size of 30–70 nm (Fig. 3a), which is consistent with the SEM observation (Fig. S4†). However, after reacting with the Cu^{2+} solution, the hexagonal structure is destroyed. The edges of the adsorbent become smoother and a new material with a smaller size is formed. According to the adsorption data, the structural change of ZIF-8 after Cu^{2+} adsorption can be presumably due to the ion exchange between Cu^{2+} and Zn^{2+}.

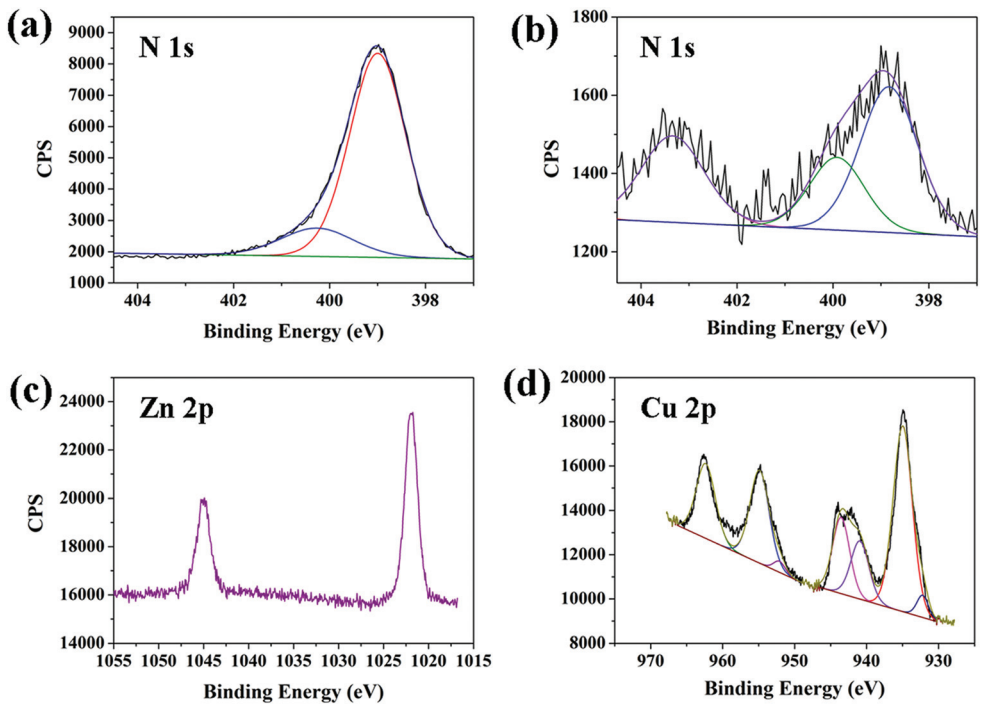

Fig. 5 N XPS spectrum of the sample before (a) and after (b) adsorption, Zn (c) and Cu (d) XPS spectrum of the sample after adsorption (Cu^{2+} concentration of 150 mg L^{-1}).

FTIR analysis. The FTIR spectra of ZIF-8 before and after the adsorption of Cu^{2+} are shown in Fig. 4. The spectra of ZIF-8 are analyzed as follows: C–N stretching on the imidazole rings, 3136 cm^{-1}; C–H stretching of $-CH_3$, 2960 and 2929 cm^{-1}; C═N stretching, 1589 cm^{-1}; Zn–N stretching, 420 cm^{-1}. After reacting with Cu^{2+} solutions, a new peak is observed at 511 cm^{-1}, which should be attributed to Cu–N stretching, indicating that Cu^{2+} has been connected onto ZIF-8 through ion exchange or the coordination reaction.

XPS analysis. XPS analysis is also used to investigate the state change of ZIF-8 before and after the adsorption of Cu^{2+} (Fig. 5). The binding energy of N 1s in ZIF-8 is about 399 and 400.3 eV, corresponding to C–N and C═N in 2-methylimidazole, respectively. After reacting with the Cu^{2+} solution, the two peaks of N 1s for 2-methylimidazole still exist, and a new peak at ~403.4 eV appears, due to the coordination reaction between the nitrogen atom and Cu^{2+}. Moreover, the peaks of Zn 2p with the binding energy of 1022 and 1045 eV still exist after the adsorption of Cu^{2+}, which means that the structure of ZIF-8 is partially preserved under these conditions. The peaks of Cu 2p appear after adsorption, demonstrating that Cu^{2+} has been adsorbed onto ZIF-8.

XRD analysis. In order to explore the reaction product when Zn^{2+} in ZIF-8 is replaced by Cu^{2+} completely, the Cu^{2+} concentration of 300 mg L^{-1} is used in the adsorption experiment and powder X-ray diffraction experiments are carried out to study the phase and structure of ZIF-8 before and after adsorption, as shown in Fig. 6a. The major sharp diffraction peaks are presented in the case of ZIF-8, which are similar to the data published in other articles,[37] indicating that the as-prepared ZIF-8 is a single pure phase without impurity. However, after reacting with the Cu^{2+} solution, almost all the peaks of ZIF-8 disappear, and a wide peak with 2θ at about 12.6° is present, which means that the structure of ZIF-8 has been completely changed by Cu^{2+} and a new complex is formed. In addition, it is found that after white ZIF-8 powders are added into the colorless aqueous solution containing Cu^{2+}, the solution turns blue (Fig. S3†), which further confirms the likely formation of the copper complex.

SEM-EDS mapping analysis. The distribution of elements for ZIF-8 before and after adsorption is also analyzed by SEM-EDS mapping. As displayed in Fig. 7a. we can see that ZIF-8 is made up of carbon, nitrogen and zinc, and these three kinds of elements are distributed adequately in ZIF-8. However, as shown in Fig. 7b, after reacting with the Cu^{2+} solution, the zinc element disappears, and copper elements appear in the solid, indicating that Zn^{2+} is replaced by Cu^{2+} completely. And a small amount of Cl and O elements appears, possibly due to the pH regulation of the solutions and the formation of cupric hydroxide, respectively.

The adsorption mechanism. From the adsorption data and various characterization results, we can deduce an adsorption mechanism for our work (Scheme 1). During the adsorption

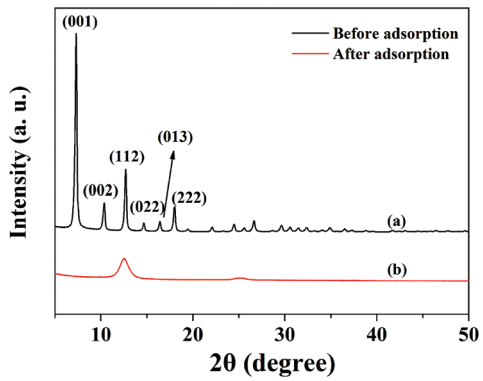

Fig. 6 Powder X-ray diffraction patterns of ZIF-8 before and after adsorption.

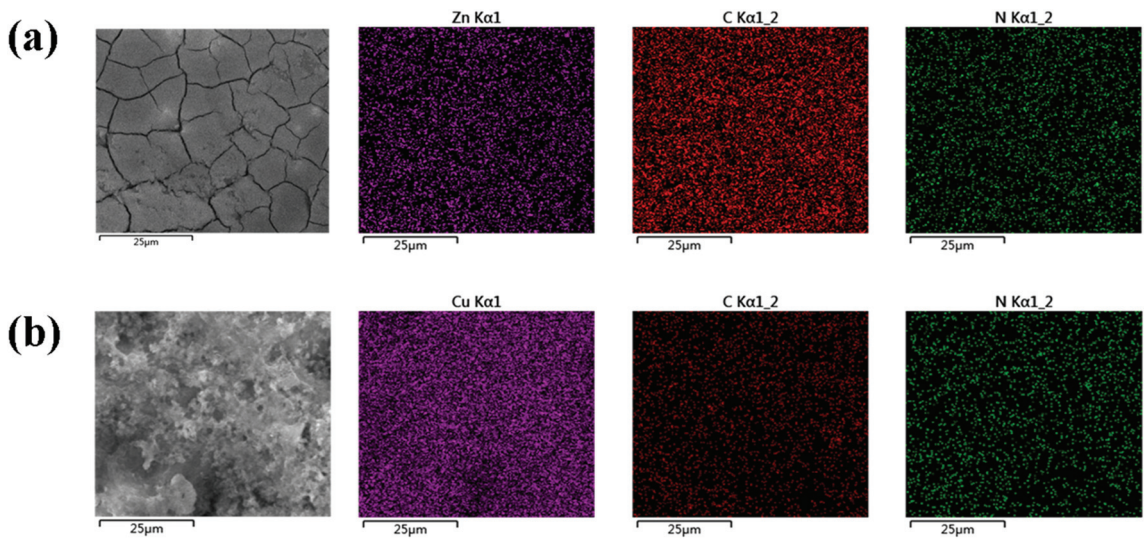

Fig. 7 SEM-EDS mapping of ZIF-8 (a) before adsorption and (b) after adsorption.

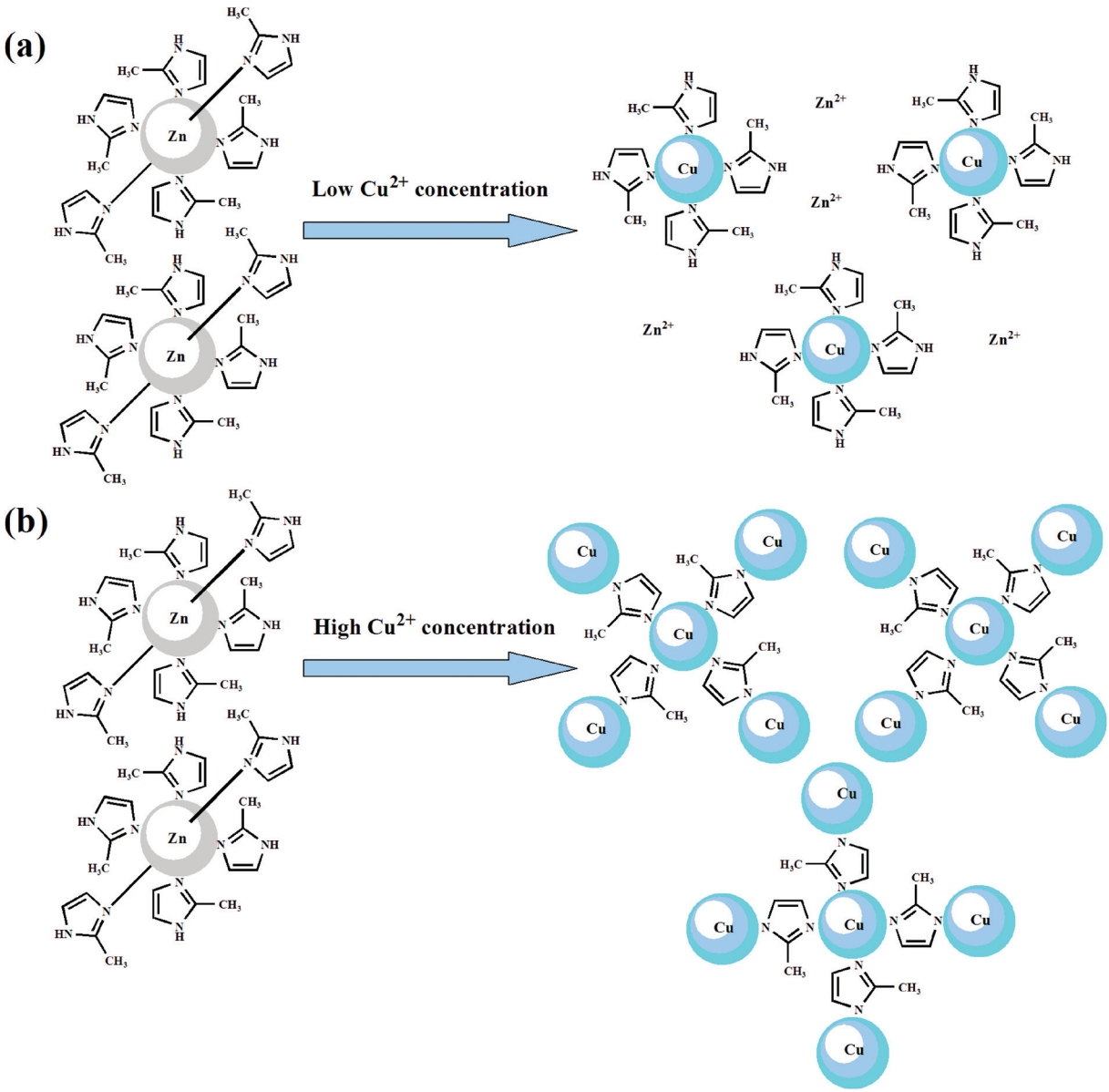

Scheme 1 The schematic showing the adsorption mechanism of Cu^{2+} in aqueous solutions by using ZIF-8 nanocrystals. (a) Ion exchange reaction at a low concentration of Cu^{2+}; (b) coordination reaction between Cu^{2+} and the nitrogen atom on 2-methylimidazole at a high concentration of Cu^{2+}.

process of Cu^{2+}, Zn^{2+} in ZIF-8 is replaced by Cu^{2+} and a new complex is formed. The reasons are: (1) the similar atomic radius between Zn and Cu, Zn^{2+} in ZIF-8 can be easily replaced by Cu^{2+}; (2) the valence electron layer structure of Zn^{2+} is more stable than that of Cu^{2+}, thus the chemical coordination ability of Cu^{2+} is stronger than that of Zn^{2+}.[43] After Zn^{2+} is replaced by Cu^{2+} completely, as shown in Scheme 1a, the adsorption amount per unit mass of ZIF-8 continuously increases due to the coordination reaction between Cu^{2+} and the nitrogen atom on 2-methylimidazole, as shown in Scheme 1b. Therefore, the adsorption process of Cu^{2+} by ZIF-8 involves ion exchange when the concentration of Cu^{2+} is lower than 200 mg L^{-1} and the coordination reaction when the concentration of Cu^{2+} is higher than 200 mg L^{-1}.

Conclusions

In this study, ZIF-8 nanocrystals are synthesized at room temperature and used as adsorbents for removal of Cu^{2+} from aqueous solutions. It is found that: (i) the pH shows little effect on the adsorption of ZIF-8 when the pH of the solution is between 3 and 6. (ii) ZIF-8 exhibits fast kinetics for highly efficient removal Cu^{2+} with an adsorption time of less than

30 min. (iii) ZIF-8 demonstrates high adsorption capacities of Cu^{2+}, about 800 mg g^{-1}, when the initial concentration of Cu^{2+} is 420 mg L^{-1}. (iv) ZIF-8 demonstrates high removal efficiency with both high and low concentrations of Cu^{2+}. (v) The adsorption mechanism involves the ion exchange process and coordination reaction.

Experimental

Chemicals

All the analytical reagent-grade chemicals we used in this work were purchased from Sinopharm Chemical Reagent Co., Ltd (Shanghai, China) without further purification. The aqueous solution of Cu (1000 mg L^{-1}) was prepared by dissolving $Cu(NO_3)_2$ in distilled water. The other concentrations were prepared by successively diluting the as-prepared initial solution. The pH of the solutions was adjusted by using NaOH or HCl. Milli-Q water (18.2 MΩ cm^{-1}) was used throughout the experiments.

Synthesis of ZIF-8 crystals

ZIF-8 crystals were prepared following a previously reported method.[31] First, 0.81 g 2-methylimidazole was mixed with 25 mL methanol; after the solid was totally dissolved in the solvent, 0.7 g $Zn(NO_3)_2{\cdot}6H_2O$ with 25 mL methanol was added into the solution. The mixture was stirred continuously for 5 h. The product solids were collected by centrifuging the mixture at 3000 rpm for 10 min and washed with methanol at least three times. The collected solid was then dried at 75 °C overnight.

Adsorption test

In a typical adsorption test, ZIF-8 was first ground into powder, and then 30 mg ZIF-8 was added into a 90 mL aqueous solution containing Cu^{2+}. The mixture was treated with ultra-sonication for 2 min and stirred for 30 min, and then separated by using a needle filter with a pore diameter of 200 microns. The rest of the heavy metals in the aqueous systems were detected and analyzed *via* ICP-OES. It should be noted that all the reported data for adsorption tests in this work were the average of at least three replicates for each experiment.

Characterization

The concentration of heavy metallic ions was determined using an inductively coupled plasma optical emission spectrometer (ICP-OES, PE Optima 2100DV, Perkin-Elmer, USA). Gas sorption analyses were conducted *via* Quantachrome Instruments Autosorb-iQ (Boynton Beach, Florida USA) with extra-high pure nitrogen. Transmission electron microscopy (TEM) images were recorded on a JEOL 2100 instrument (JEOL, Japan) with an acceleration voltage of 200 kV. For TEM analysis, the samples were prepared by drop casting the dispersions onto carbon-coated copper grids, which were air-dried subsequently. Fourier transform infrared spectroscopy (FTIR) data were collected in the wavenumber ranging from 4000 to 400 cm^{-1} on a Nicolet 6700 Fourier-transform infrared spectrometer using KBr pellets. X-ray photoelectron spectrometry (XPS) was carried out using an AXIS Ultra DLD instrument with Mg Kα radiation as the X-ray source and all the binding energies were referenced to the C 1s peak at 284.8 eV The phase structure of ZIF-8 before and after adsorption was analyzed on an X-ray diffractometer (XRD, D8 Advance, Bruker AXS, Germany). The morphology and chemical distribution of the samples were analysed using a field emission scanning electron microscope (FESEM) (TM-1000, Hitachi, Japan). For XPS, SEM and XRD analysis, the samples were prepared by drop casting the dispersions onto a silicon pellet (for XPS and SEM) and a glass plate (for XRD), which were subsequently dried in a closed dryer.

Acknowledgements

This work is supported by the Project for Science and Technology Service of Chinese Academy of Sciences (KFJ-SW-STS-172), the National Natural Science Foundation of China (U1507104), the aided program for Science and Technology Innovative Research Team of Ningbo Municipality (Grant No.: 2014B82010, and 2015B11002), the Zhejiang Provincial Natural Science Foundation of China (Grant No. R5110230), the Hundred Talents Program of Chinese Academy of Sciences (2010-735), and the Chevron Innovative Research Fund (CIRS) and Economic Development Assistantship (EDA) at Louisiana State University.

References

1 L. Chabaane, S. Tahiri, A. Albizane, M. El Krati, M. L. Cervera and M. de la Guardia, *Chem. Eng. J.*, 2011, **174**, 310–317.
2 R. Dutta, S. S. Mohammad, S. Chakrabarti, B. Chaudhuri, S. Bhattacharjee and B. K. Dutta, *Water Environ. Res.*, 2010, **82**, 138–146.
3 M. Ajmal, R. A. K. Rao and M. A. Khan, *J. Hazard. Mater.*, 2005, **122**, 177–183.
4 S. Larous, A. H. Meniai and M. B. Lehocine, *Desalination*, 2005, **185**, 483–490.
5 N. Bakhtiari, S. Azizian, S. M. Alshehri, N. L. Torad, V. Malgras and Y. Yamauchi, *Microporous Mesoporous Mater.*, 2015, **217**, 173–177.
6 Q. Y. Chen, Z. Luo, C. Hills, G. Xue and M. Tyrer, *Water Res.*, 2009, **43**, 2605–2614.
7 M. Gharabaghi, M. Irannajad and A. R. Azadmehr, *Ind. Eng. Chem. Res.*, 2012, **51**, 954–963.
8 M. Y. Vilensky, B. Berkowitz and A. Warshawsky, *Environ. Sci. Technol.*, 2002, **36**, 1851–1855.
9 S. M. C. Ritchie, K. E. Kissick, L. G. Bachas, S. K. Sikdar, C. Parikh and D. Bhattacharyya, *Environ. Sci. Technol.*, 2001, **35**, 3252–3258.

10 R. Celis, M. C. Hermosin and J. Cornejo, *Environ. Sci. Technol.*, 2000, **34**, 4593–4599.
11 U. Wingenfelder, C. Hansen, G. Furrer and R. Schulin, *Environ. Sci. Technol.*, 2005, **39**, 4606–4613.
12 G. Yuvaraja, M. V. Subbaiah and A. Krishnaiah, *Ind. Eng. Chem. Res.*, 2012, **51**, 11218–11225.
13 M. Kobya, E. Demirbas, E. Senturk and M. Ince, *Bioresour. Technol.*, 2005, **96**, 1518–1521.
14 K. Kadirvelu, C. Faur-Brasquet and P. Le Cloirec, *Langmuir*, 2000, **16**, 8404–8409.
15 C. Y. Lu and H. S. Chiu, *Chem. Eng. Sci.*, 2006, **61**, 1138–1145.
16 C. S. Lu, H. Chiu and C. T. Liu, *Ind. Eng. Chem. Res.*, 2006, **45**, 2850–2855.
17 Y. H. Li, S. G. Wang, Z. K. Luan, J. Ding, C. L. Xu and D. H. Wu, *Carbon*, 2003, **41**, 1057–1062.
18 L. S. Zhong, J. S. Hu, H. P. Liang, A. M. Cao, W. G. Song and L. J. Wan, *Adv. Mater.*, 2006, **18**, 2426–2431.
19 T. Phuengprasop, J. Sittiwong and F. Unob, *J. Hazard. Mater.*, 2011, **186**, 502–507.
20 Z. X. Jin, H. Y. Gao and L. H. Hu, *RSC Adv.*, 2015, **5**, 88520–88528.
21 L. S. Zhong, J. S. Hu, A. M. Cao, Q. Liu, W. G. Song and L. J. Wan, *Chem. Mater.*, 2007, **19**, 1648–1655.
22 L. S. Zhong, J. S. Hu, L. J. Wan and W. G. Song, *Chem. Commun.*, 2008, **10**, 1184–1186.
23 X. Xu, J. Park, Y. K. Hong and A. M. Lane, *Mater. Chem. Phys.*, 2015, **152**, 9–12.
24 X. Xu, J. Park, Y. K. Hong and A. M. Lane, *J. Solid State Chem.*, 2015, **222**, 84–89.
25 X. Xu, J. Park, Y. K. Hong and A. M. Lane, *Mater. Lett.*, 2015, **144**, 119–122.
26 Z. Q. Xie, J. Q. Zhao and Y. Wang, *Electrochim. Acta*, 2015, **174**, 1023–1029.
27 M. P. Suh, H. J. Park, T. K. Prasad and D. W. Lim, *Chem. Rev.*, 2012, **112**, 782–835.
28 L. E. Kreno, K. Leong, O. K. Farha, M. Allendorf, R. P. Van Duyne and J. T. Hupp, *Chem. Rev.*, 2012, **112**, 1105–1125.
29 A. M. Shultz, O. K. Farha, J. T. Hupp and S. T. Nguyen, *J. Am. Chem. Soc.*, 2009, **131**, 4204–4205.
30 P. Horcajada, R. Gref, T. Baati, P. K. Allan, G. Maurin, P. Couvreur, G. Ferey, R. E. Morris and C. Serre, *Chem. Rev.*, 2012, **112**, 1232–1268.
31 Z. Q. Xie, Z. Y. He, X. H. Feng, W. W. Xu, X. D. Cui, J. H. Zhang, C. Yan, M. A. Carreon, Z. Liu and Y. Wang, *ACS Appl. Mater. Interfaces*, 2016, **8**, 10324–10333.
32 X. D. Cui, Z. Q. Xie and Y. Wang, *Nanoscale*, 2016, **8**, 11984–11992.
33 F. Ke, L. G. Qiu, Y. P. Yuan, F. M. Peng, X. Jiang, A. J. Xie, Y. H. Shen and J. F. Zhu, *J. Hazard. Mater.*, 2011, **196**, 36–43.
34 Y. Wang, G. Q. Ye, H. H. Chen, X. Y. Hu, Z. Niu and S. Q. Ma, *J. Mater. Chem.*, 2015, **3**, 15292–15298.
35 Y. Zhang, X. Zhao, H. Huang, Z. Li, D. Liu and C. Zhong, *RSC Adv.*, 2015, **5**, 72107–72112.
36 Z. Q. Wang, M. Wang, G. H. Wu, D. Y. Wu and A. G. Wu, *Dalton Trans.*, 2014, **43**, 8461–8468.
37 L. Zhang, G. Qian, Z. J. Liu, Q. Cui, H. Y. Wang and H. Q. Yao, *Sep. Purif. Technol.*, 2015, **156**, 472–479.
38 C. G. Lee, J. W. Jeon, M. J. Hwang, K. H. Ahn, C. Park, J. W. Choi and S. H. Lee, *Chemosphere*, 2015, **130**, 59–65.
39 L. Trakal, R. Sigut, H. Sillerova, D. Faturikova and M. Komarek, *Arabian J. Chem.*, 2014, **7**, 43–52.
40 M. R. Awual, *Chem. Eng. J.*, 2015, **266**, 368–375.
41 S. T. Yang, Y. L. Chang, H. F. Wang, G. B. Liu, S. Chen, Y. W. Wang, Y. F. Liu and A. N. Cao, *J. Colloid Interface Sci.*, 2010, **351**, 122–127.
42 M. A. Tofighy and T. Mohammadi, *J. Hazard. Mater.*, 2011, **185**, 140–147.
43 V. S. Mummidivarapu, S. Bandaru, D. S. Yarramala, K. Samanta, D. S. Mhatre and C. P. Rao, *Anal. Chem.*, 2015, **87**, 4988–4995.